MODELING OF UH-60A HUB ACCELERATIONS WITH NEURAL NETWORKS

Sesi Kottapalli
Aeromechanics Branch
Army/NASA Rotorcraft Division
NASA Ames Research Center
Moffett Field, California

Summary

Neural network relationships between the full-scale, flight test hub accelerations and the corresponding three N/rev pilot floor vibration components (vertical, lateral, and longitudinal) are studied. The present quantitative effort on the UH-60A Black Hawk hub accelerations considers the lateral and longitudinal vibrations. An earlier study had considered the vertical vibration. The NASA/Army UH-60A Airloads Program flight test database is used. A physics based "maneuver-effect-factor (MEF)," derived using the roll-angle and the pitch-rate, is used. Fundamentally, the lateral vibration data show high vibration levels (up to 0.3 g's) at low airspeeds (for example, during landing flares) and at high airspeeds (for example, during turns). The results show that the advance ratio and the gross weight together can predict the vertical and the longitudinal vibration. However, the advance ratio and the gross weight together cannot predict the lateral vibration. The hub accelerations and the advance ratio can be used to satisfactorily predict the vertical, lateral, and longitudinal vibration. The present study shows that neural network based representations of all three UH-60A pilot floor vibration components (vertical, lateral, and longitudinal) can be obtained using the hub accelerations along with the gross weight and the advance ratio. The hub accelerations are clearly a factor in determining the pilot vibration. The present conclusions potentially allow for the identification of neural network relationships between the experimental hub accelerations obtained from wind tunnel testing and the experimental pilot vibration data obtained from flight testing. A successful establishment of the above neural network based link between the wind tunnel hub accelerations and the flight test vibration data can increase the value of wind tunnel testing.

Notation

MEF	Maneuver effect factor, Equation 1
MISO	Multiple-input, single-output

N	Number of main rotor blades, N = 4 for the UH-60A
N/rev	Integer (N) multiple of main rotor speed
PLATV	Peak, 4P pilot floor lateral vibration, g's
PLATV-related	Refers to those hub acceleration values that occur at time t = τ, where τ is the time at which the peak lateral vibration PLATV occurs
PLONGV	Peak, 4P pilot floor longitudinal vibration, g's
PLONGV-related	Refers to those hub acceleration values that occur at time t = τ, where τ is the time at which the peak longitudinal vibration PLONGV occurs
PVV	Peak, 4P pilot floor vertical vibration, g's
PVV-related	Refers to those hub acceleration values that occur at time t = τ, where τ is the time at which the peak vertical vibration PVV occurs
R	Linear regression correlation, an R close to 1 indicates that a regression-based relationship exists between the test data and the neural network predictions
RMS error	Root mean square error between the test data and the neural network predictions, g's

Introduction

For helicopters, the relationships between the rotor hub accelerations and the fuselage vibration may be linear or nonlinear and involve many variables. Here, fuselage

vibration is defined as the N/rev fuselage acceleration at the pilot location. For the UH-60A flight test data that were considered in Ref. 1, one of the conclusions was that the fuselage vibration trends qualitatively matched those of the hub accelerations. Reference 1 did not present any quantitative representations for the hub accelerations. Also, in Ref. 1, the relationships between the hub accelerations and the fuselage vibrations were not quantified.

Neural networks can provide links between the hub accelerations and the fuselage vibration, and these links may be linear or nonlinear. The neural network based study reported in Ref. 2 represented the first systematic effort that considered the UH-60A hub accelerations in a quantitative manner, and also identified numerical relationships between the hub accelerations and the pilot floor vertical vibrations. Also, Ref. 2 was undertaken to obtain a better understanding of the basic dynamics underlying the main rotor-dependent pilot vertical vibration and the associated hub accelerations.

The present study considers the other two linear vibration components, namely, the lateral and the longitudinal components, and thus completes the modeling of all three components of the UH-60A pilot floor vibration. The ability to predict the pilot vibration using the advance ratio and the gross weight is studied. This study builds up on previous neural network studies that were conducted at NASA Ames in the areas of rotorcraft performance, acoustics, and dynamics (Refs. 2 to 5). Flight test data from the NASA/Army UH-60A Airloads Program (Refs. 6 and 7) are used.

The present use of neural networks is justified because neural networks can perform multi-dimensional, nonlinear curve fitting. This feature is useful in this study that seeks to identify smoothly varying relationships. This work is considered to be a generic methodology and is not specific to the UH-60A configuration under consideration.

Objectives

This neural network based modeling (or representation) study involves the helicopter N/rev peak, pilot floor lateral vibration (PLATV) and the longitudinal vibration (PLONGV), and also considers the corresponding hub accelerations. Reference 2 had considered the pilot floor vertical vibration (PVV). The present study has the following three objectives:

1. Create two UH-60A in-plane vibration databases containing the PLATV data, and separately, the PLONGV data.

2. Corresponding to the above two databases for PLATV and PLONGV, create two different databases containing the appropriate hub accelerations. The

section on Hub Acceleration and Pilot Vibration Databases contains a discussion on the present methodology used to obtain the appropriate hub accelerations.

3. Assess the data quality of the hub accelerations and obtain their neural network based representations.

4. Using the hub accelerations and flight condition parameters such as the advance ratio and the gross weight, determine whether reasonably accurate neural network based models of PLATV and PLONGV can be obtained.

Hub Acceleration and Pilot Vibration Databases

The source of the hub accelerometer data was the NASA/Army UH-60A Airloads Program flight test database (Refs. 6 and 7). For purposes of this dynamics related study, the following categories of flights from Refs. 6 and 7 are considered: "Steady and Maneuvering Airloads" and "Maneuvers." The following flight conditions are included: level flight, rolls, pushovers, pull-ups, autorotations, and landing flares. These conditions approximate the entire UH-60A flight envelope.

The UH-60A hub accelerometers were mounted on a triaxial block glued to the main rotor shaft 4.5 inches from the center of rotation (Ref. 1). Three accelerometers (radial, tangential, and vertical) were used. Following Ref. 1, the tangential accelerometer measurements were used to present the in-plane response because it has a smaller centrifugal acceleration value than the radial sensor.

In general, to obtain a time varying, step-by-step simulation of the pilot vibration during a maneuver, a neural network based time-series method can be used. However, such methods are complex. In the present, initial modeling study using neural networks, a static-mapping approach involving the peak vibration level is followed. This implies that each flight condition is characterized by its peak vibration. The possibility of utilizing the peak-vibration-based static mapping in a quasi-static manner to simulate time varying maneuvers was investigated in Ref. 5. A quasi-static approach will not capture all dynamic effects, and may miss the prediction of relevant maximums and their associated phases. Also, a time-series analysis using neural networks will capture the maximums and phases more accurately, compared to a quasi-static approach. The present study considers the 3P and 5P tangential hub accelerations and the 4P vertical hub acceleration. The appropriate hub acceleration values are taken as those corresponding to the peak pilot floor vibration under consideration, namely, PLATV or PLONGV. For

example, let the peak lateral vibration PLATV occur at a time t = τ. The hub accelerations at time t = τ are defined as the corresponding or appropriate hub accelerations. The above hub acceleration values are referred to as the "PLATV-related" hub accelerations.

Maneuver Effect Factor

The MEF, a non-dimensional parameter, is used to characterize helicopter maneuvers involving simultaneous non-zero roll-angle and pitch-rate, and the MEF is used as one of the neural network inputs. The MEF is derived by a consideration of the vertical force changes arising because of the roll-angle and the pitch-rate. The changes in the lift due to both the roll-angle and the acceleration due to the pitch-rate are accounted for. The MEF is subsequently defined by the following equation:

Maneuver effect factor, MEF =
$$[1 \, / \cos (\text{roll-angle})] \, *$$
$$[\, 1 + (\text{pitch-rate} * \text{airspeed} \, / \, g) \,]$$

(1)

where "g" is the acceleration due to gravity. The purpose of the MEF is to compactly represent complex maneuvers using a single, physics-based parameter. Depending on the reference axes system used, other parameters can be derived, and this would result in slightly different formulations.

The number of the neural network training data points in the present study is over 200. These points represent the entire database. Each training data point represents a single flight condition. The maximum advance ratio is 0.48. The gross weight range encountered is from 14,749 lbs to 17,720 lbs. Approximately 25% of the training database involves maneuver related points. Here, maneuver related refers to a flight condition for which the maneuver effect factor MEF is not equal to 1.

Basic Variations: Hub Accelerations and Pilot Vibration

Pilot Vibration

Figures 1-3 show the variations of the pilot floor vibration components PVV, PLATV, and PLONGV versus the advance ratio. The data shown in Figs. 1-3 use the above mentioned 200 point flight database. Thus, in addition to the variation in the advance ratio covered in the figures, overall, these data involve variations in the gross weight, the main rotor RPM, the density ratio, the MEF, and the ascent/descent rate (and variations in the cyclic and collective stick positions). The PVV was considered earlier in Ref. 2, and its variation (Fig. 1) is included in this paper for completeness. The other two pilot floor vibration components, namely, PLATV (Fig.

2) and PLONGV (Fig. 3) are considered in this paper. In Fig. 2, high pilot floor lateral vibration levels (up to 0.3 g's) can be seen at low airspeeds (for example, during landing flares) and at high airspeeds (for example, during turns).

Hub Accelerations

Figure 4 shows the PLATV-related 3P tangential hub acceleration variation with the advance ratio. These data were obtained with the 3P bifilars installed on the UH-60A. In Fig. 4, the low speed "hump" due to rotor wake effects can be seen around an advance ratio of 0.09 (approximately 40 knots). Figure 5 shows the PLATV-related 5P tangential hub acceleration variation with the advance ratio. Compared to the 3P hub acceleration data in Fig. 4, the 5P hub acceleration data in Fig. 5 appear to contain more scatter. This could be due to the fact that the 3P bifilars bring in a forced response behavior that tends to smooth out the 3P accelerations. In the UH-60A Airloads Program, the UH-60A did not have 5P bifilars installed. Figure 6 shows the PLATV-related 4P vertical hub acceleration variation with the advance ratio. Figures 7-9 show the corresponding PLONGV-related hub acceleration variations versus the advance ratio.

Neural Network Approach

To accurately capture the required functional dependencies, the neural network inputs must be carefully selected and account for all important physical traits that are specific to the application. The important attributes of a neural network are its type (radial-basis function network, back-propagation network, recurrent network, etc.) and its complexity (i.e., the number of processing elements (PEs) and the number of hidden layers). The present overall neural network modeling approach is based on the approach followed in Refs. 2-5. The back-propagation type of network with a hyperbolic tangent as the basis function, and the extended-delta-bar-delta (EDBD) algorithm as the learning rule (Ref. 8) is used.

The number of neural network PEs required depends on the specific application. The determination of the appropriate number of PEs is done by starting with a minimum number of PEs. Additional PEs are added to improve neural network performance by reducing the RMS error between the test data and the neural network predictions. Typically, five PEs are added at each step in this process. Adding two or three PEs at a time refines the neural network. A more automated method of determining the optimum neural network architecture would be desirable, and this subject is an active area of research.

If the correlation plot, comparing measured and predicted values, shows only small deviations from the 45-deg reference line, the neural network has produced an

acceptable representation of the subject test data. If the plot shows points well off of the 45-deg line, poor quality test data may exist in the database. A detailed examination of the subject test database is then required to identify the source(s) of the errors associated with any poor quality test data. The analyst should not solely rely on the neural network based correlation procedure to eliminate poor quality test data. This procedure, however, contributes to data assessment, and two examples from previous studies are briefly discussed as follows. First, in Ref. 3 (Figs. 11 and 12 in Ref. 2) the above procedure was applied to experimental tilt-rotor blade flatwise bending moments. In the Ref. 3 example, the subject test data points were not repeatable, possibly due to instrumentation problems. Second, in Ref. 4 (Fig. 1 in Ref. 4) the above procedure was applied to experimental wind tunnel tilt-rotor noise data. In the Ref. 4 example, the conclusion was that the presence of gusty winds, affecting the wind tunnel flow quality (flow unsteadiness) and the thrust coefficient, might have adversely affected the quality of the subject data. In the present initial study, the PLATV and PLONGV correlation points well off of a +/- 0.05 g's error band are further examined for poor quality.

For the notation used in this paper, a neural network architecture such as "4-25-5-1" refers to a neural network with four inputs, twenty five processing elements (PEs) in the first hidden layer, five PEs in the second hidden layer, and one output. The present application of neural networks to full-scale helicopter flight test vibration and hub accelerations data has been conducted using the neural networks package NeuralWorks Pro II/PLUS (version 5.3) by NeuralWare (Ref. 8). The PLATV and PLONGV vibration components are considered separately in this neural network based modeling study.

Results

The neural network results presented in this section are based on the entire 200 point database. This study separately considers the in-plane vibration components (PLATV, PLONGV). The vertical vibration component (PVV) was considered in Ref. 2. For comparative purposes and for completeness, selected PVV results from Ref. 2, with details omitted, are included in the present paper. The neural network details for the PVV are not given in this paper (see Ref. 2).

Exploratory Study on Pilot Vibration

The objective here is to determine whether the advance ratio and the gross weight can predict the three vibration components. Three different MISO 2-10-5-1 back-propagation neural networks are used (one for each of the three vibration components). The advance ratio and the gross weight are the two inputs, and the vibration component under consideration (PVV or PLATV or PLONGV) is the single output. The PVV training details (Ref. 2) are not included in this paper. For PLATV, the above back-propagation network has been trained for 5 million iterations with resulting R = 0.81 and RMS error = 0.04 g's. For PLONGV, the above back-propagation network has been trained for approximately 5 million iterations with resulting R = 0.91 and RMS error = 0.02 g's.

Figures 10-12 show the resulting correlation plots for the PVV, PLATV, and PLONGV, respectively. Figures 10 and 12 show that the advance ratio and the gross weight can reasonably predict the PVV (Fig. 10) and the PLONGV (Fig. 12) for the entire flight database, maneuvers included, despite the fact that the advance ratio and the gross weight do not account for maneuver effects. Figure 11 shows that the advance ratio and the gross weight cannot predict the PLATV. The PLATV result (Fig. 11) is in contrast to that obtained for the PVV (Fig. 10) and the PLONGV (Fig. 12).

Compared to the above neural network based model that uses two inputs, the following neural network based model involves far more input variables, and uses six inputs. In the present study, correlation results based on a more complex physical model that accounts for maneuver effects (and other effects noted below) are also considered. Three different MISO 6-10-5-1 back-propagation neural networks are used (one for each of the three vibration components). The six inputs are as follows: the advance ratio, the gross weight, the main rotor RPM, density ratio, the MEF, and the ascent/descent rate. For PLATV, the above back-propagation network has been trained for 4 million iterations with resulting R = 0.97 and RMS error = 0.02 g's. For PLONGV, the back-propagation network has been trained for 4 million iterations with resulting R = 0.97 and RMS error = 0.01 g's.

Figures 13-15 show the correlation results for the PVV, PLATV, and PLONGV, respectively, based on the above six inputs, including the MEF. Figures 13-15 show correlations that are acceptable. In the present quasi-static approach, the flight test time history variations are represented by their average values over an 8-revolution segment length. Figure 16 shows the resulting time histories of the vertical, lateral, and longitudinal vibration components during an unsteady pull-up at 120 knots. The vertical vibration peak occurs first, followed by the lateral and the longitudinal vibration peaks. Figures 17-19 show the successful, quasi-static modeling of the time varying vibration for a pull-up maneuver at 120 knots. The above predictions have been obtained by introducing appropriate time offsets that give the best fits. Such fidelity in predicting the pilot floor vibrations shows considerable promise in using neural networks to obtain the UH-60A fuselage vibrations.

4

Representation of Hub Accelerations

In the present study, the quality of the hub accelerations flight test data has been assessed, and numerical representations of the flight test data have been obtained. There are six neural network inputs which are the same as those used for the above MEF-based correlation. These inputs are given as follows: the advance ratio, the gross weight, the main rotor RPM, the density ratio, the MEF, and the ascent/descent rate. The three neural network outputs are as follows: the 3P and 5P tangential hub accelerations and the 4P vertical hub acceleration. Two different MIMO 6-15-5-3 back-propagation neural networks are used for the PVV-related and PLONGV-related hub accelerations. A single MIMO 6-15-10-3 back-propagation neural network is used for the PLATV-related hub accelerations. The above PLATV-related and PLONGV-related back-propagation networks have been trained for 5 million iterations. The PVV-related hub accelerations results are not shown here and can be found in Ref. 2. Figures 20-22 show the correlation plots for the PLATV-related hub accelerations. Figures 23-25 show the correlation plots for the PLONGV-related hub accelerations. The PLATV-related and PLONGV-related hub acceleration results are given as follows.

PLATV-Related Hub Accelerations. For the 3P tangential hub acceleration correlation (Fig. 20), R = 0.95 and RMS error = 0.04 g's. For the 5P tangential hub acceleration correlation (Fig. 21), R = 0.95 and RMS error = 0.05 g's. For the 4P vertical hub acceleration correlation (Fig. 22), R = 0.93 and RMS error = 0.04 g's.

PLONGV-Related Hub Accelerations. For the 3P tangential hub acceleration correlation (Fig. 23), R = 0.90 and RMS error = 0.06 g's. For the 5P tangential hub acceleration correlation (Fig. 24), R = 0.90 and RMS error = 0.06 g's. For the 4P vertical hub acceleration correlation (Fig. 25), R = 0.90 and RMS error = 0.04 g's.

Overall, the hub acceleration flight test "data quality" is assessed as being acceptable. There are no identifiable poor quality data points such as those discussed earlier (Neural Network Approach). As noted in Ref. 3, the analyst should not solely rely on the neural network based correlation to eliminate poor quality test data. The present process does, however, contribute to data assessment. Finally, the present results imply that for the UH-60A, numerical relationships (the identification model) relating the hub accelerations to the flight condition parameters have been obtained.

Relationships Between Hub Accelerations and Pilot Vibration

The objective is to represent the pilot floor vibration components using the 3P and 5P tangential hub accelerations and the 4P vertical hub acceleration as the three core inputs. The vibration component under consideration (PVV or PLATV or PLONGV) is the single neural network output. For each vibration component, three cases are created, with their inputs listed as follows:

Case 1 inputs: the three hub accelerations (3 input case). Depending on the vibration component under consideration (PVV or PLATV or PLONGV), the hub accelerations that are used are identified as follows, respectively: PVV-related or PLATV-related or PLONGV-related.

Case 2 inputs: the three hub accelerations and the advance ratio (4 input case).

Case 3 inputs: the three hub accelerations, the advance ratio and the gross weight (5 input case).

Results for the lateral vibration component and the longitudinal vibration component (PLATV and PLONGV, respectively) are presented below. The vertical vibration component (PVV) was studied in Ref. 2 using the same input lists as in Cases 1-3 above. For comparative purposes and for completeness, the PVV results from Ref. 2, with details omitted, are included in the present paper.

Case 1 Results. Three different MISO 3-10-5-1 back-propagation neural networks are used (one for each of the three vibration components). As noted above, the relevant three hub accelerations are the inputs. For PLATV and PLONGV, the above back-propagation networks have been trained for 5 million iterations. For PLATV, R = 0.66 and the RMS error = 0.05 g's. For PLONGV, R = 0.72 and the RMS error = 0.03 g's. Figures 26-28 show the correlation plots for the PVV, the PLATV, and the PLONGV using the Case 1 inputs. Figures 26-28 show that there does not appear to exist a unique relationship between the hub accelerations and the pilot vibration components. At the same time, it can be suggested that the hub accelerations inherently contain some basic information that depends on the flight condition.

Case 2 Results. Three different MISO 4-10-5-1 back-propagation neural networks were used (one for each of the three vibration components). The three hub accelerations and the advance ratio are the inputs. For PLATV and PLONGV, the above back-propagation networks have been trained for 5 million iterations. For PLATV, R = 0.96 and the RMS error = 0.02 g's. For PLONGV, R = 0.96 and the RMS error = 0.01 g's. Figures 29-31 show the correlation plots for the PVV, the PLATV, and the PLONGV using the Case 2 inputs. Figures 29-31 show that the hub accelerations and the advance ratio can represent the pilot floor vibration. This correlation is very encouraging because it appears that, for all airspeeds, the physics of the pilot vibration variation

with airspeed is being captured by the advance ratio (in combination with the hub accelerations). This result is encouraging also because both the hub accelerations and the advance ratio are parameters that can be easily measured. Since the hub accelerations are measured in the rotating system, it is necessary to use slip rings to transfer the hub accelerations data to the fixed system.

Case 3 Results. Three different MISO 5-10-6-1 back-propagation neural networks are used (one for each of the three vibration components). The three hub accelerations along with the advance ratio and the gross weight are the inputs. For PLATV and PLONGV, the above back-propagation network has been trained for 5 million iterations. For PLATV, R = 0.97 and the RMS error = 0.02 g's. For PLONGV, R = 0.96 and the RMS error = 0.01 g's. Figures 32-34 show the correlation plots for the PVV, the PLATV, and the PLONGV using the Case 3 inputs. Figures 32-34 show that the hub accelerations along with the advance ratio and the gross weight can represent the pilot vibration. Overall, compared to the Case 2 correlation (involving the hub accelerations and the advance ratio, Figs. (29-31), the Case 3 correlation (Figs. 32-34) is not surprising. This is because the hub accelerations may contain substantial basic information and very little additional information (e.g., the advance ratio) is required to produce neural network based representations. Also, the correlation shown in Figs. 13-15 use the maneuver effect factor MEF whereas the correlation shown in Figs. 32-34 use the hub accelerations (along with the advance ratio and the gross weight). In the present study, both correlation results are obtained such that they fall within a +/- 0.05 g's error band and thus are comparable to each other. Hence, it can be suggested that the hub accelerations contain maneuver effects information reflecting load factor effects.

Selected results are shown in Tables 1-3 in numerical form to show typical neural network predictions. The flight test vibrations for four specific flight conditions and the corresponding four sets neural network based vibrations are shown in Tables 1-3 (presented later in this paper). The neural network models for which the predictions were obtained are noted in the three tables. These models are as follows: the MEF model and the hub accelerations along with advance ratio and the gross weight model. To summarize, it can be directly observed from Tables 1-3 that the present neural network based models are accurate to within +/- 0.05 g's of the corresponding flight test values for high-speed level flight, descent, climb, and a constant turn flight condition.

Neural Network Validation

The full UH-60A Airloads Program database has been explored till now for modeling the PLATV and the PLONGV and the hub accelerations using the present,

neural network related entire database (200 point database). If additional data were available beyond the 200 point database, then these data could have been used to test (validate) the neural networks. The neural networks could have been applied to other operating conditions. However, additional data are not available. Consequently, the validation of the neural networks is done by working with the entire 200 point database, and splitting it into a training database and a testing (validation) database, and subsequently verifying that the testing results are acceptable. Approximately 80% of the entire database's 200 points are used to create a training database and the remaining approximately 20% are used to create a separate testing database. The PLATV and PLONGV neural network validation results are summarized as follows (the corresponding PVV neural network validation results were summarized in Ref. 2). In the following, the *training RMS error* refers to the RMS error obtained for the case that has been trained using "80% of the entire database." This 80%-training database represents a "new training database" (as compared to the entire database ("100%") that has been used till now for training, Results section). The testing RMS error refers to the RMS error obtained for the case that has been tested using the remaining "20% of the entire database."

For cases with the PLATV as the single output (Figs. 14, 30, and 33), the PLATV training RMS error is ≤ 0.02 g's (with R ranging from 0.96 to 0.97). The PLATV testing RMS error is ≤ 0.04 g's (with R ranging from 0.71 to 0.91). Additionally, two sample validation (testing) plots, with the PLATV as the single output, are presented in Figs. 35a-35b. These two validation cases are associated with two important correlations that have been considered earlier, namely, those shown in Figs. 14 and 33, respectively. In the first sample validation case there are six inputs, listed as follows: the advance ratio, the gross weight, the main rotor RPM, density ratio, the MEF, and the ascent/descent rate. The corresponding validation plot is shown in Fig. 35a (R = 0.91, RMS error = 0.03 g's). In the second sample validation case there are five inputs, listed as follows: the three hub accelerations along with the advance ratio and the gross weight. The corresponding validation plot is shown in Fig. 35b (R = 0.71, RMS error = 0.04 g's). The above validation results prove that the neural networks presently used to model the PLATV have predictive capability.

For cases with the PLONGV as the single output (Figs. 15, 31, and 34), the PLONGV training RMS error is ≤ 0.01 g's (with R ranging from 0.96 to 0.98). The PLONGV testing RMS error is ≤ 0.03 g's (with R ranging from 0.72 to 0.93). Additionally, two sample validation (testing) plots, with the PLONGV as the single output, are presented in Figs. 36a-36b. These two validation cases are associated with two important correlations that have been considered earlier, namely, those shown in Figs. 15 and 34, respectively. In the first

sample validation case there are six inputs, listed as follows: the advance ratio, the gross weight, the main rotor RPM, density ratio, the MEF, and the ascent/descent rate. The corresponding validation plot is shown in Fig. 36a (R = 0.93, RMS error = 0.02 g's). In the second sample validation case there are five inputs, listed as follows: the three hub accelerations along with the advance ratio and the gross weight. The corresponding validation plot is shown in Fig. 36b (R = 0.73, RMS error = 0.03 g's). The above validation results prove that the neural networks presently used to model the PLONGV have predictive capability.

Validation results for the PLATV-related and PLONGV-related hub accelerations are given in Tables 4-5 below.

Table 4. Training ("80%") Error and Testing ("20%") Error for PLATV-related Hub Accelerations (associated with Figs. 20-22)

	Training		Testing	
Hub Accel.	R	RMS error	R	RMS error
3P Tang.	0.97	0.03 g's	0.75	0.06 g's
5P Tang.	0.96	0.05 g's	0.80	0.07 g's
4P Vert.	0.97	0.03 g's	0.57	0.08 g's

Table 5. Training ("80%") Error and Testing ("20%") Error for PLONGV-related Hub Accelerations (associated with Figs. 23-25)

	Training		Testing	
Hub Accel.	R	RMS error	R	RMS error
3P Tang.	0.90	0.06 g's	0.88	0.04 g's
5P Tang.	0.91	0.06 g's	0.81	0.06 g's
4P Vert.	0.93	0.04 g's	0.54	0.08 g's

Finally, the above validation results for the pilot vibration and the hub accelerations prove that the neural networks used in the present study have predictive capability.

Concluding Remarks

Full-scale, flight test based peak, 4P pilot floor lateral and longitudinal vibrations (PLATV and PLONGV, respectively) and the corresponding hub accelerations are considered in this initial study for modeling purposes. The present quantitative effort represents the first systematic study involving hub accelerations and the in-plane pilot floor vibrations. The flight conditions considered in the present study are as follows: level flight, rolls, pushovers, pull-ups, autorotations, and landing flares. The PLATV and PLONGV variations are considered separately. The corresponding pilot floor

vertical vibration (PVV) was considered in Ref. 2. Specific conclusions are as follows:

1) The advance ratio and the gross weight can be used to represent the peak, 4P pilot floor vertical vibration (PVV) and the peak, 4P pilot floor longitudinal vibration (PLONGV) of virtually the entire UH-60A Airloads Program database.

2) In contrast to conclusion 1 above, the advance ratio and the gross weight together cannot be used to represent the peak, 4P pilot floor lateral vibration (PLATV).

3) The quality of the hub accelerations data has been found acceptable.

4) The hub accelerations data have been successfully modeled using the following six inputs: the advance ratio, the gross weight, the main rotor RPM, the density ratio, the MEF, and the ascent/descent rate.

5) The relationships between the hub accelerations and the pilot floor vibration have been studied, and the resulting conclusions are as follows:

   a) The hub accelerations alone cannot represent the pilot floor vibration.

   b) The hub accelerations along with the advance ratio can be used to represent the pilot floor vibration. This is very encouraging since both the hub accelerations and the advance ratio are parameters that can be easily measured. Since the hub accelerations are measured in the rotating system, it is necessary to use slip rings to transfer the hub accelerations data to the fixed system.

   c) The hub accelerations along with the advance ratio and the gross weight can be used to represent the pilot floor vibration.

The focus of the future work is discussed as follows. Practically, the present results involving hub accelerations potentially allow for the identification of neural network relationships between the experimental hub accelerations obtained from wind tunnel testing and the experimental pilot floor vibration data obtained from flight testing. A successful establishment of the above neural network based link between the wind tunnel hub accelerations and the flight test vibration data can increase the value of wind tunnel testing.

References

1. Studebaker, K., "A Survey of Hub Vibration for the UH-60A Airloads Research Aircraft," American Helicopter Society International Aeromechanics

Specialists Conference, San Francisco, California, January 1994.

2. Kottapalli, S., "Neural Network Based Representation of UH-60A Pilot and Hub Accelerations," scheduled for publication in the January 2002 issue of the *Journal of the American Helicopter Society*. American Helicopter Society Aeromechanics Specialists' Meeting, Atlanta, Georgia, November 2000.

3. Kottapalli, S., "Neural Network Research on Validating Experimental Tilt-Rotor Performance," *Journal of the American Helicopter Society*, Vol. 45, No. 3, pp. 199-206, July 2000.

4. Kottapalli, S. and Kitaplioglu, C., "Neural Network Representation of Experimental Tilt-Rotor Noise," 6th AIAA/CEAS Aeroacoustics Conference, AIAA-2000-1924, Maui, Hawaii, June 2000.

5. Kottapalli, S., "Neural-Network-Based Modeling of Rotorcraft Vibration for Real-Time Applications," AIAA Modeling and Simulation Technologies Conference, AIAA-2000-4305, Denver, Colorado, August 2000.

6. Kufeld, R.M., Balough, D.L., Cross, J.L., Studebaker, K.F., Jennison, C.D., and Bousman, W.G., "Flight Testing of the UH-60A Airloads Aircraft," American Helicopter Society 50th Annual Forum, Washington, D.C., May 1994.

7. Bondi, M.J. and Bjorkman, W.S., "TRENDS, A Flight Test Relational Database," User's Guide and Reference Manual, NASA TM 108806, June 1994.

8. NeuralWorks Pro II/PLUS Manuals, NeuralWare, Inc., Pittsburgh, Pennsylvania, 1995.

Table 1. Neural Network Based Results for PVV, g's

Flight Condition	Flight Test	Maneuver-Effect-Factor (Fig. 13)	Hub Accels. + Advance-Ratio + Gross Weight (Fig. 32)
Level flight, 135 knots	0.10	0.10	0.11
Descent, 160 knots	0.25	0.24	0.26
Climb, 62 knots	0.12	0.12	0.12
Turn, 45 deg, 120 knots	0.13	0.18	0.14

Table 2. Neural Network Based Results for PLATV, g's

Flight Condition	Flight Test	Maneuver-Effect-Factor (Fig. 14)	Hub Accels. + Advance-Ratio + Gross Weight (Fig. 33)
Level flight, 135 knots	0.03	0.02	0.06
Descent, 160 knots	0.07	0.05	0.07
Climb, 62 knots	0.04	0.04	0.07
Turn, 45 deg, 120 knots	0.08	0.06	0.09

Table 3. Neural Network Based Results for PLONGV, g's

Flight Condition	Flight Test	Maneuver-Effect-Factor (Fig. 15)	Hub Accels. + Advance-Ratio + Gross Weight (Fig. 34)
Level flight, 135 knots	0.04	0.05	0.05
Descent, 160 knots	0.18	0.17	0.19
Climb, 62 knots	0.04	0.03	0.04
Turn, 45 deg, 120 knots	0.10	0.11	0.08
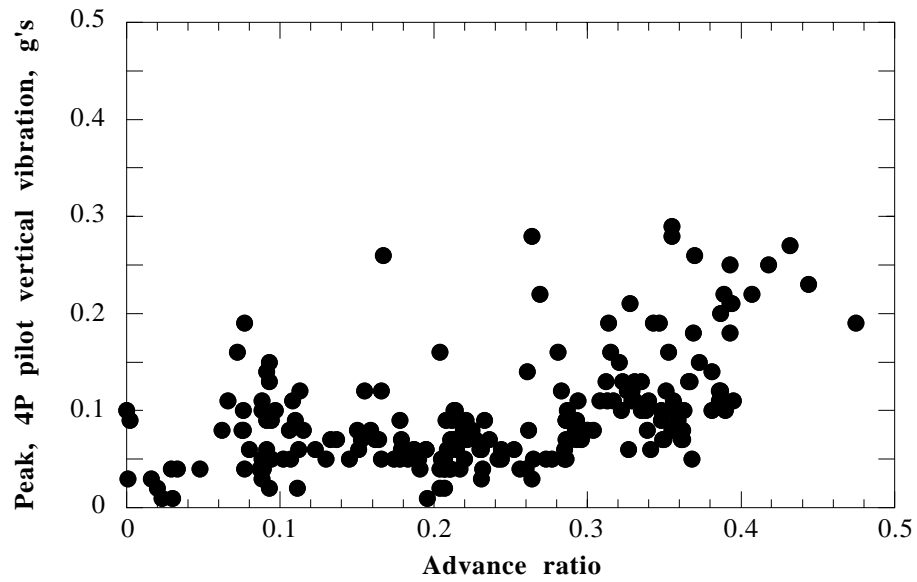
Fig. 1. UH-60A peak, 4P pilot floor vertical vibration, PVV, variation with advance ratio.
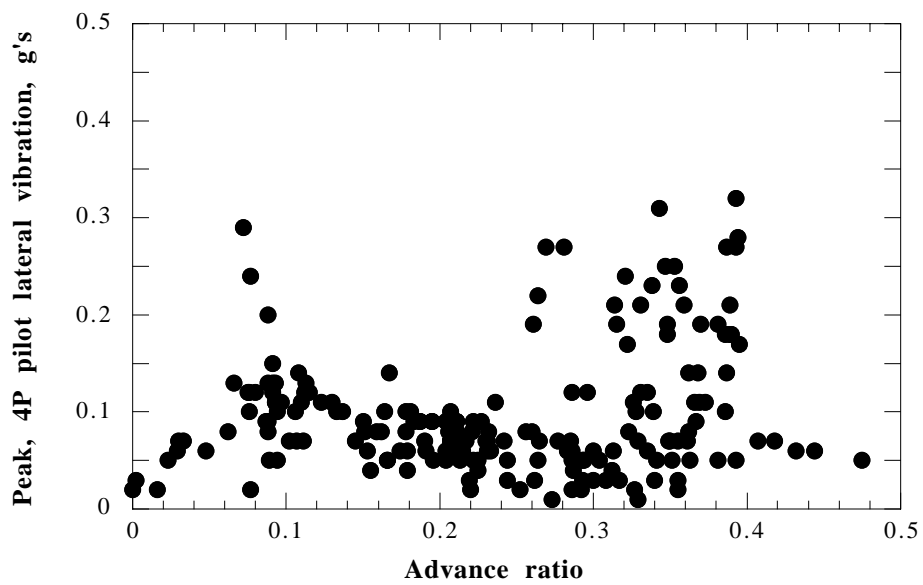
Fig. 2. UH-60A peak, 4P pilot floor lateral vibration, PLATV, variation with advance ratio.
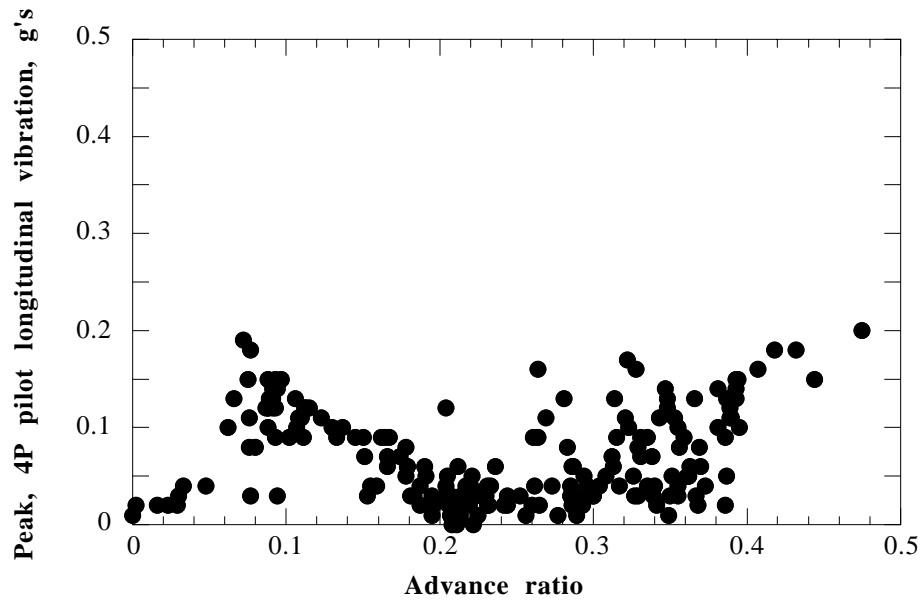
Fig. 3. UH-60A peak, 4P pilot floor longitudinal vibration, PLONGV, variation with advance ratio.
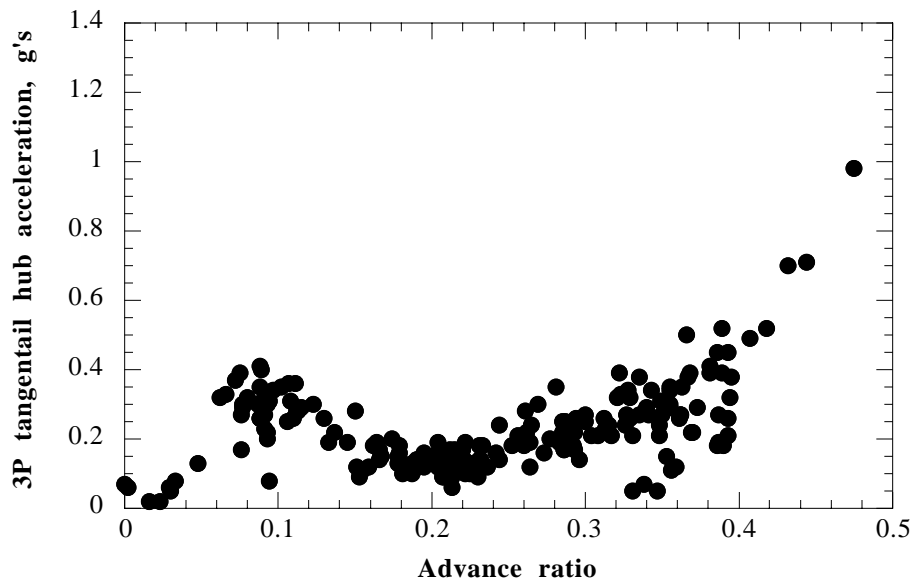
Fig. 4. UH-60A 3P tangential hub acceleration variation with advance ratio, PLATV-related.
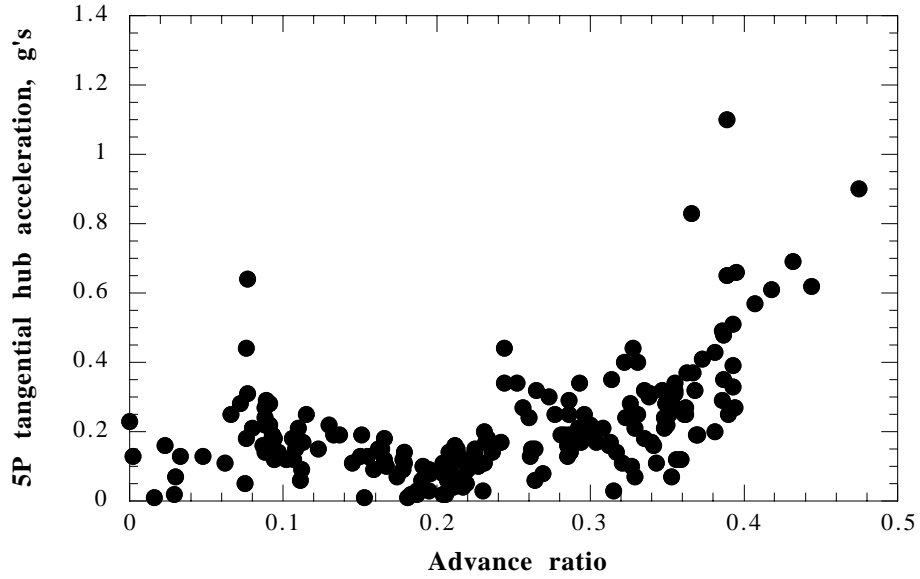
Fig. 5. UH-60A 5P tangential hub acceleration variation with advance ratio, PLATV-related.
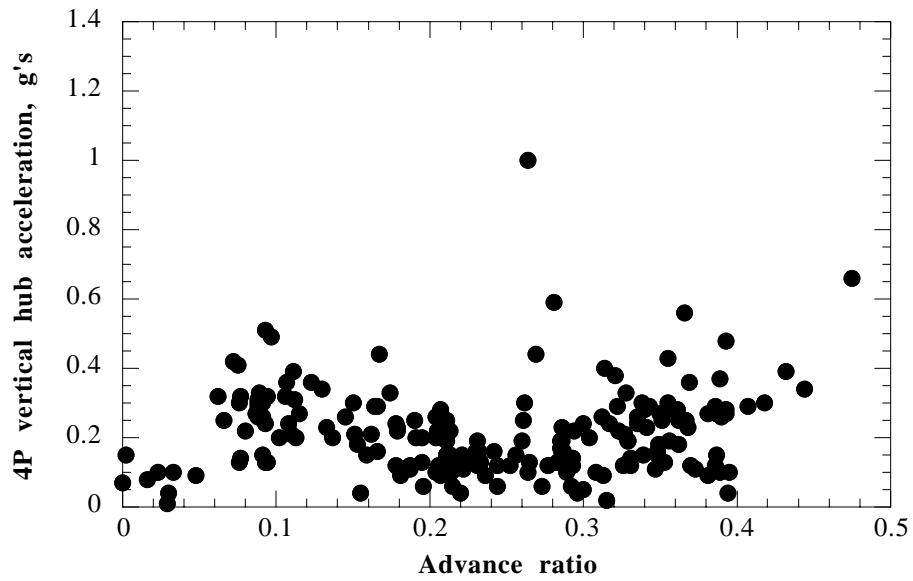
Fig. 6. UH-60A 4P vertical hub acceleration variation with advance ratio, PLATV-related.
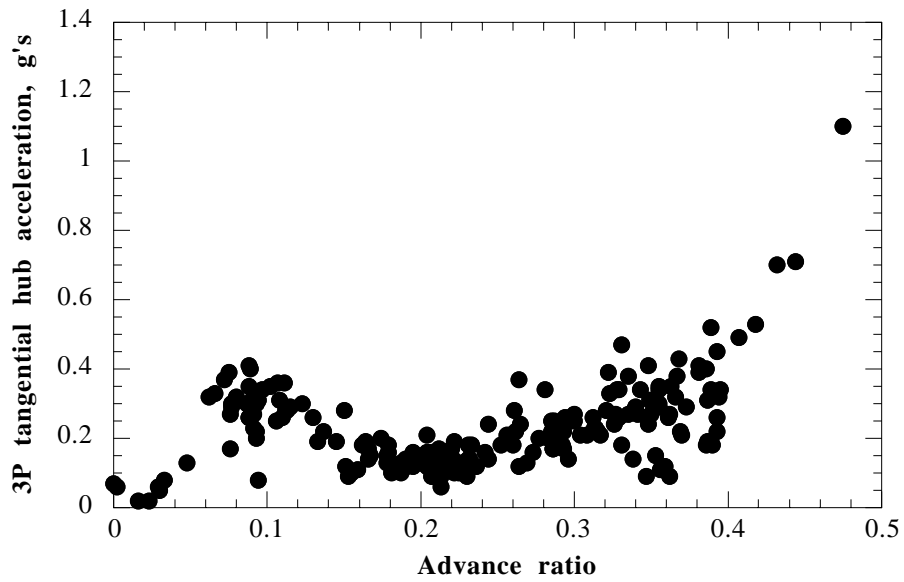
Fig. 7. UH-60A 3P tangential hub acceleration variation with advance ratio, PLONGV-related.
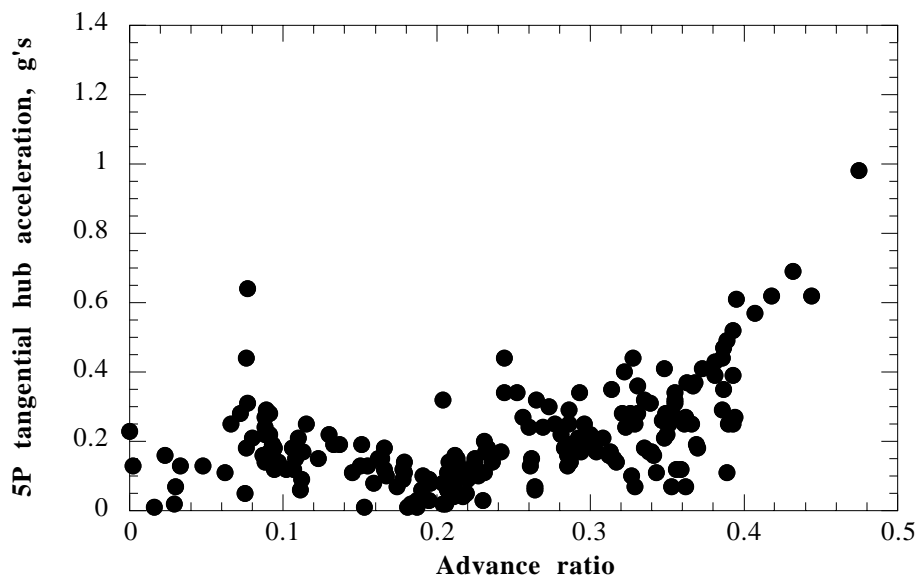
Fig. 8. UH-60A 5P tangential hub acceleration variation with advance ratio, PLONGV-related.

13
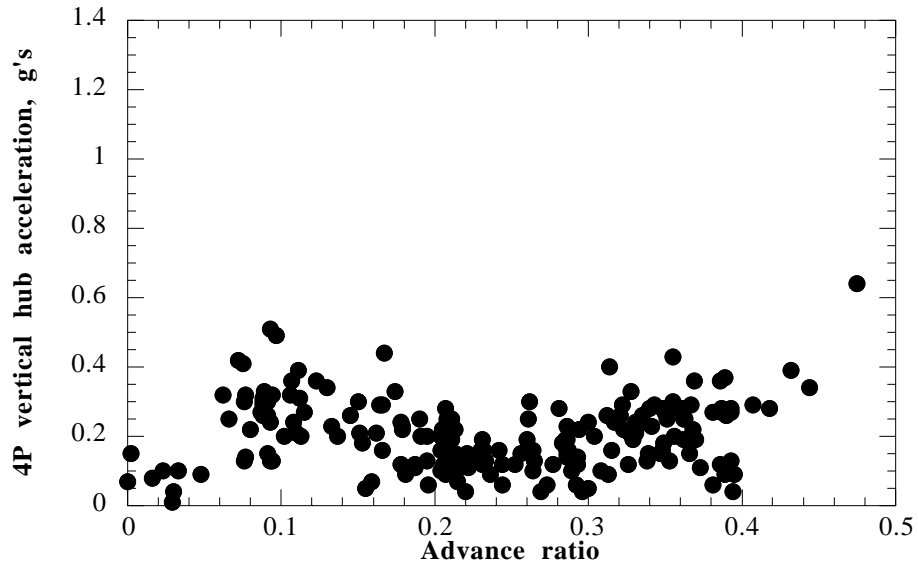
Fig. 9. UH-60A 4P vertical hub acceleration variation with advance ratio, PLONGV-related.
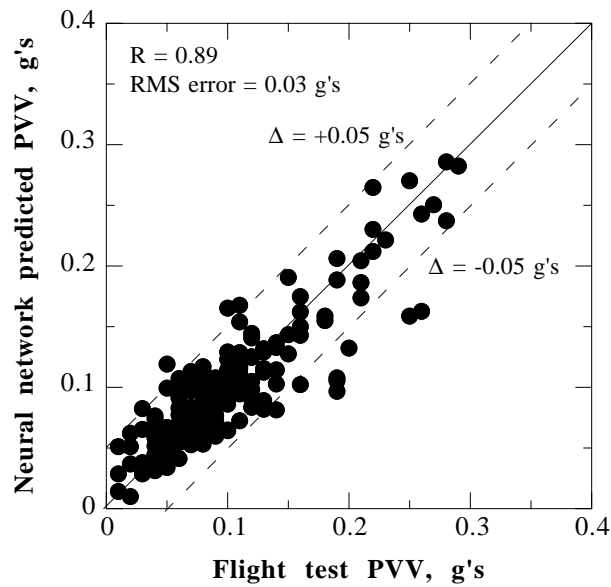
Fig. 10. PVV correlation using advance ratio and gross weight.

14
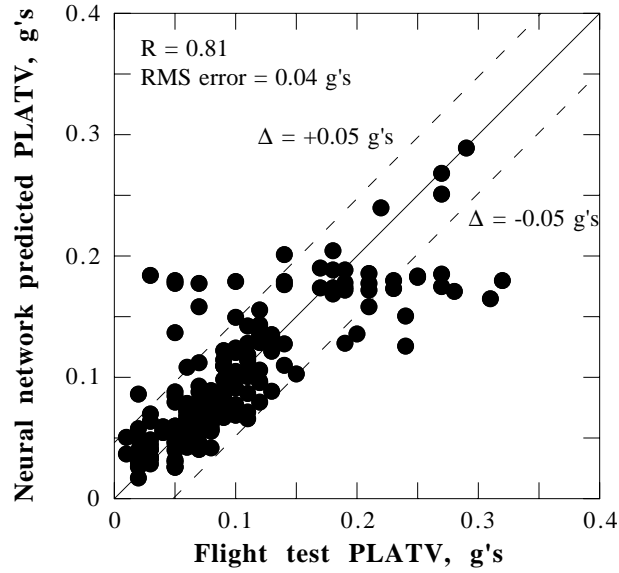
Fig. 11. PLATV correlation using advance ratio and gross weight.
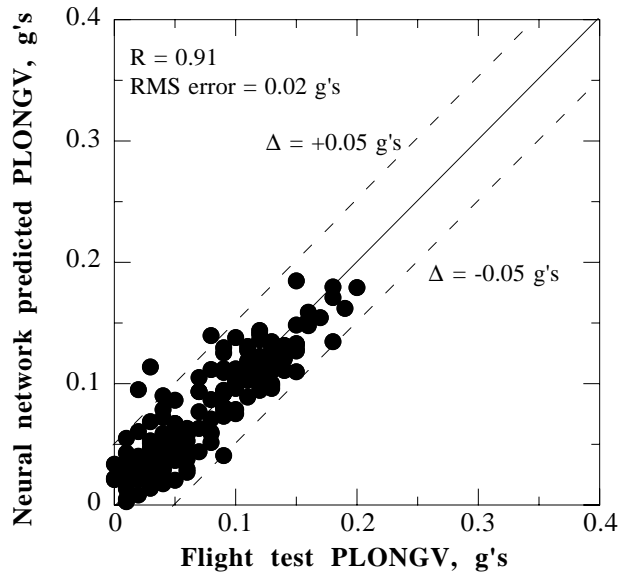
Fig. 12. PLONGV correlation using advance ratio and gross weight.
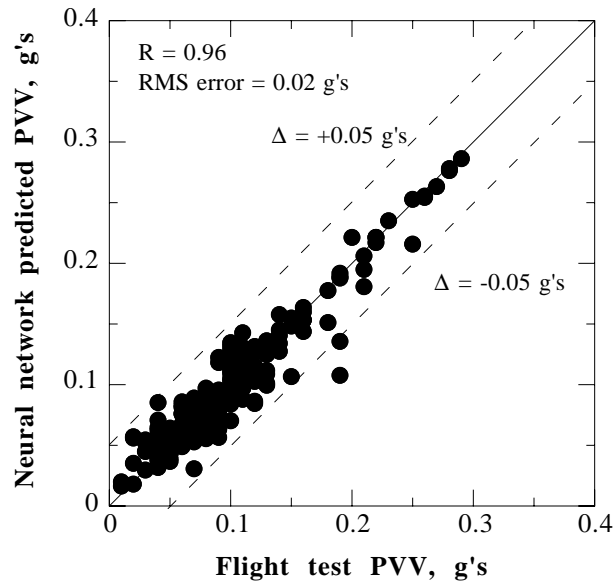
Fig. 13. PVV correlation using maneuver effect factor, MEF.
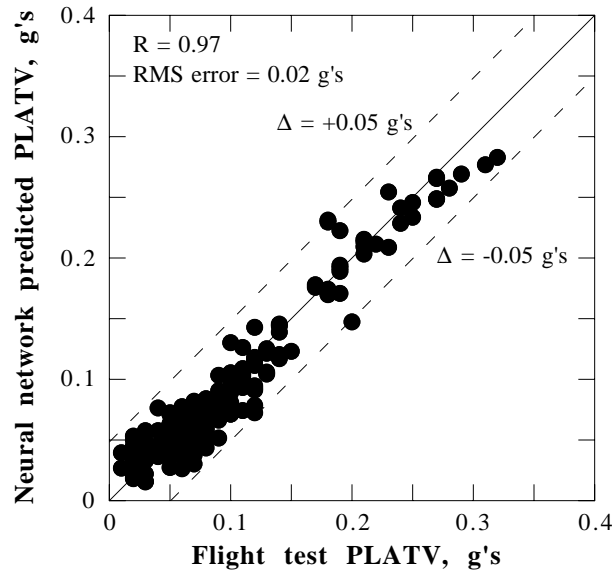
Fig. 14. PLATV correlation using maneuver effect factor, MEF.

16
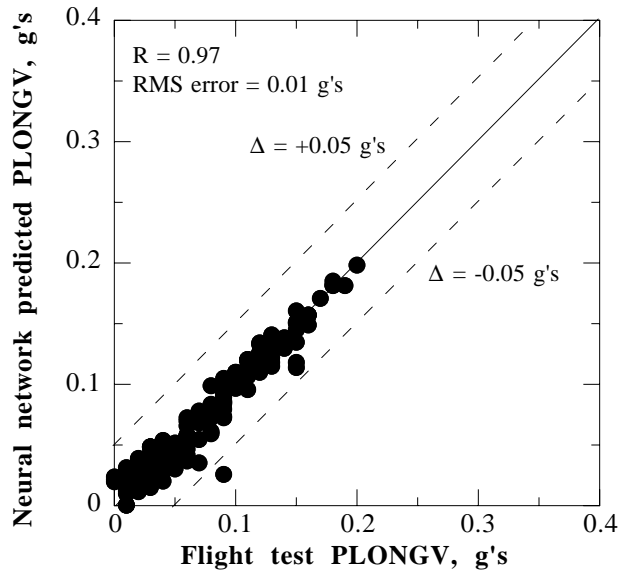
Fig. 15. PLONGV correlation using maneuver effect factor, MEF.
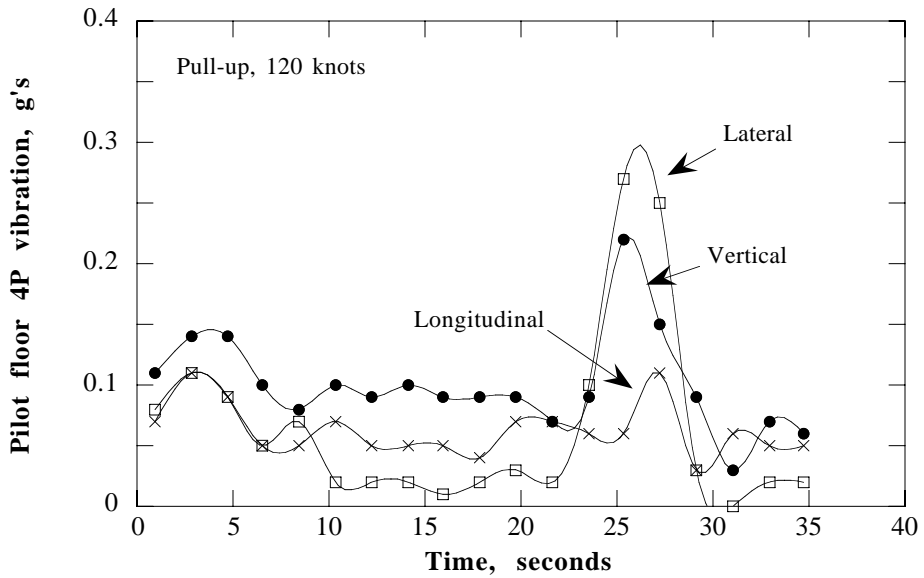
Fig. 16. Time histories of the three vibration components, pull-up, flight test.
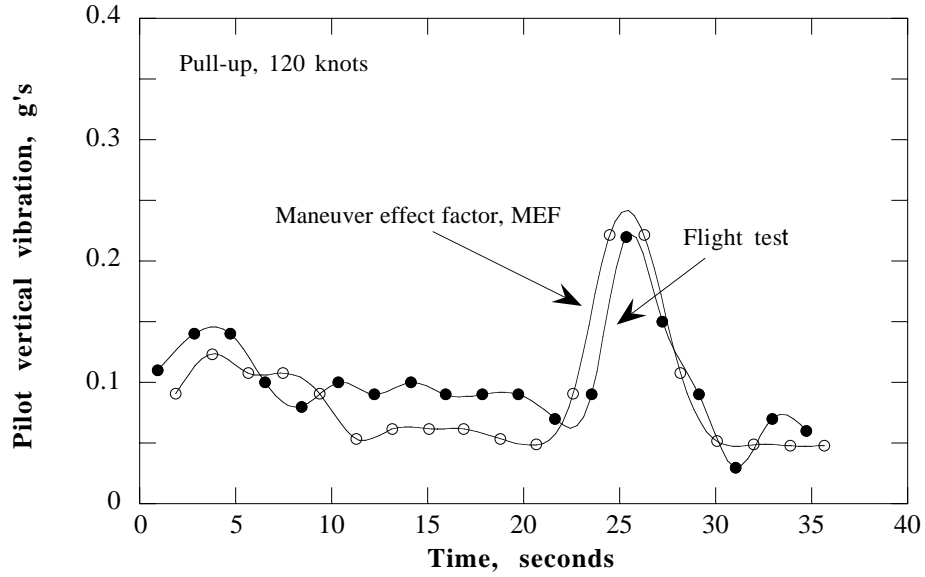
Fig. 17. Quasi-static prediction of vertical vibration using MEF.
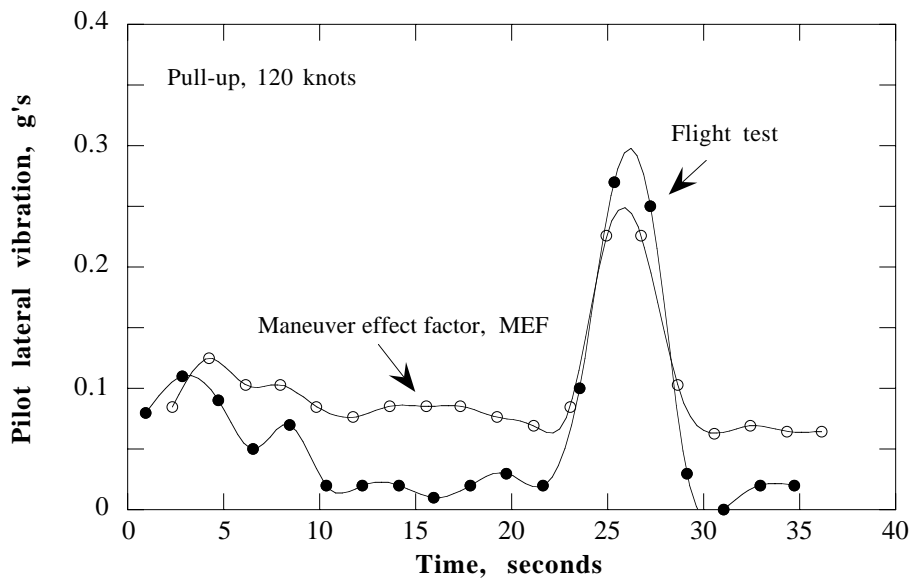
Fig. 18. Quasi-static prediction of lateral vibration using MEF.
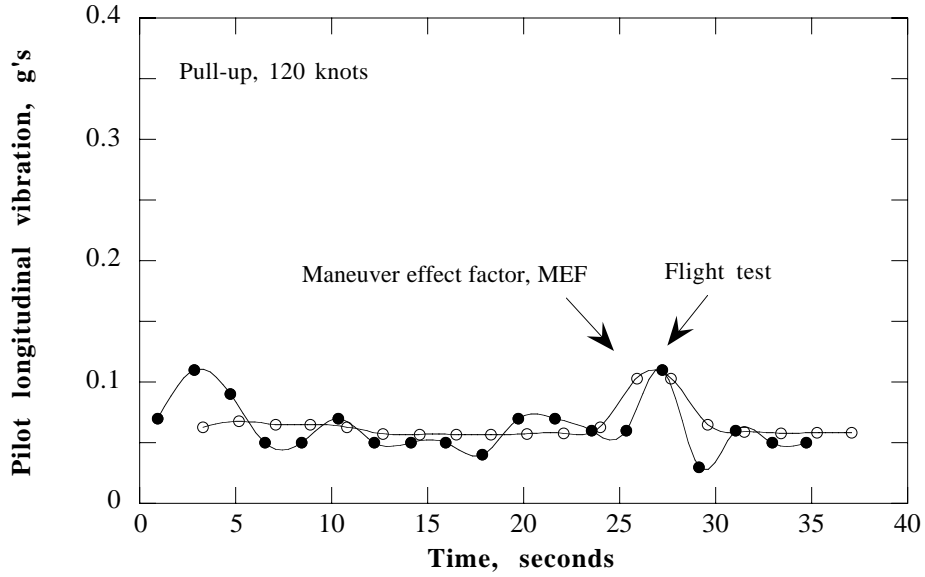
Fig. 19. Quasi-static prediction of longitudinal vibration using MEF.
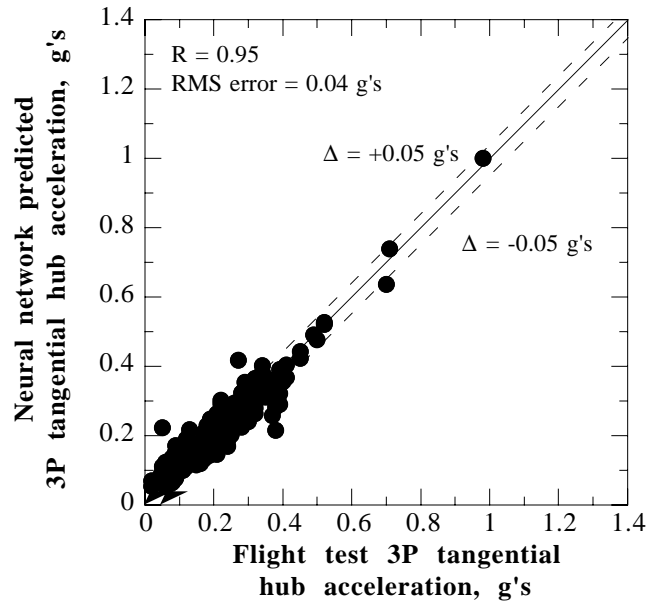
Fig. 20. 3P tangential hub acceleration correlation, PLATV-related.
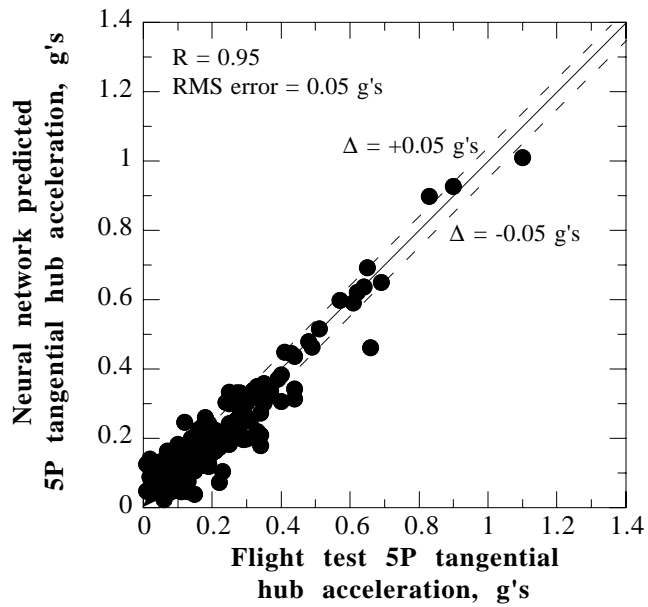
Fig. 21. 5P tangential hub acceleration correlation, PLATV-related.
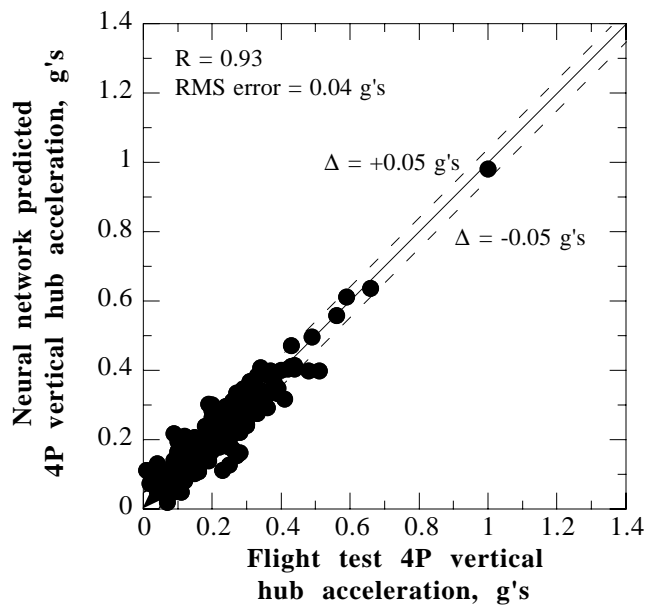
Fig. 22. 4P vertical hub acceleration correlation, PLATV-related.
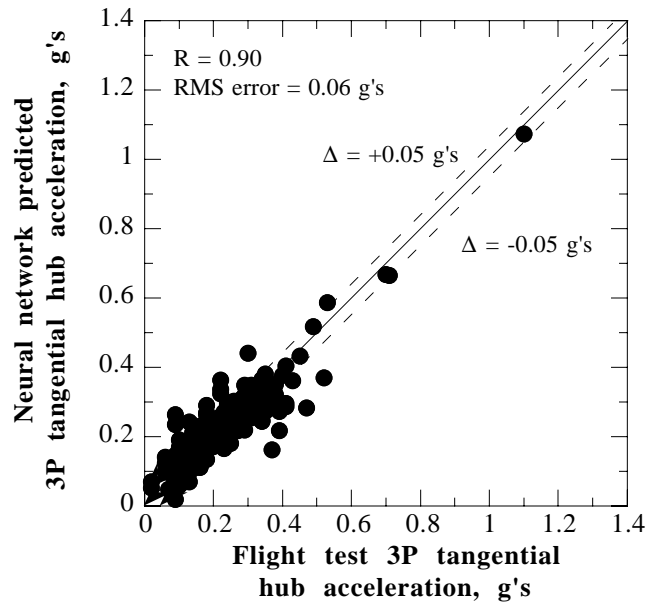
Fig. 23.   3P tangential hub acceleration correlation, PLONGV-related.
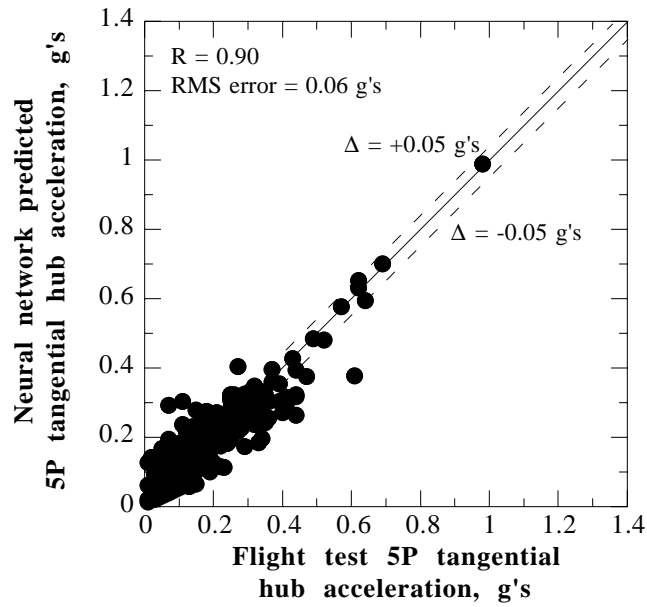
Fig. 24. 5P tangential hub acceleration correlation, PLONGV-related.
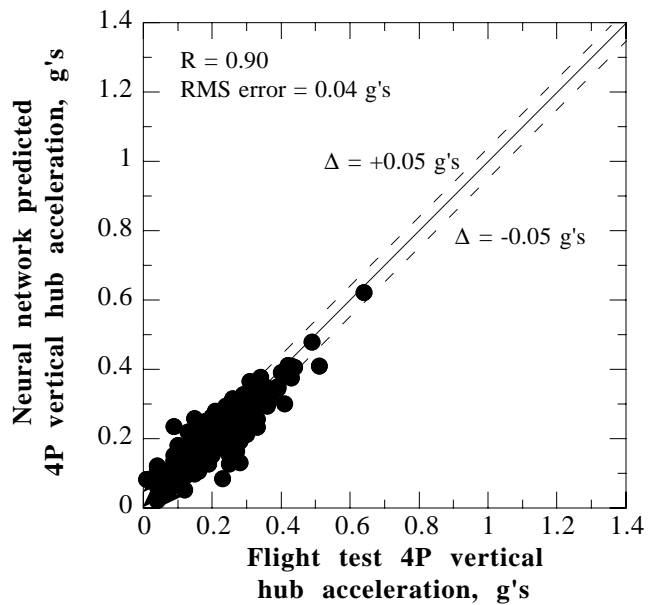
Fig. 25. 4P vertical hub acceleration correlation, PLONGV-related.
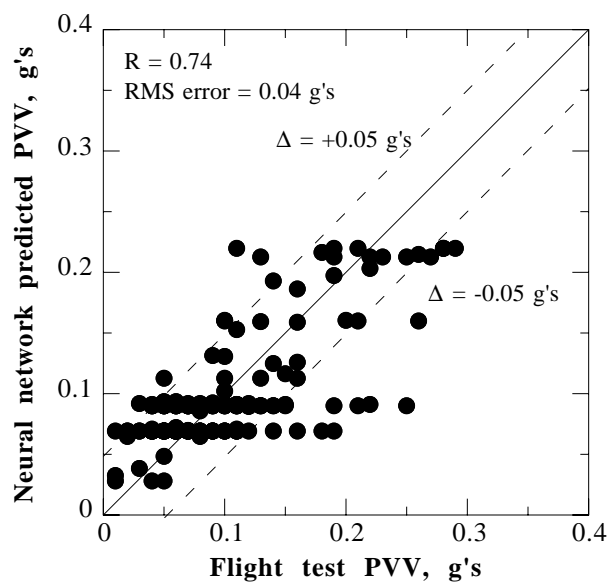
Fig. 26. PVV correlation using hub accelerations.
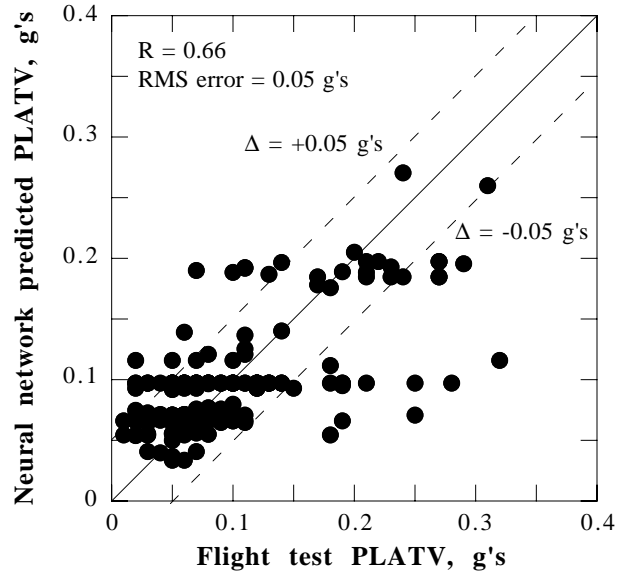
Fig. 27. PLATV correlation using hub accelerations.
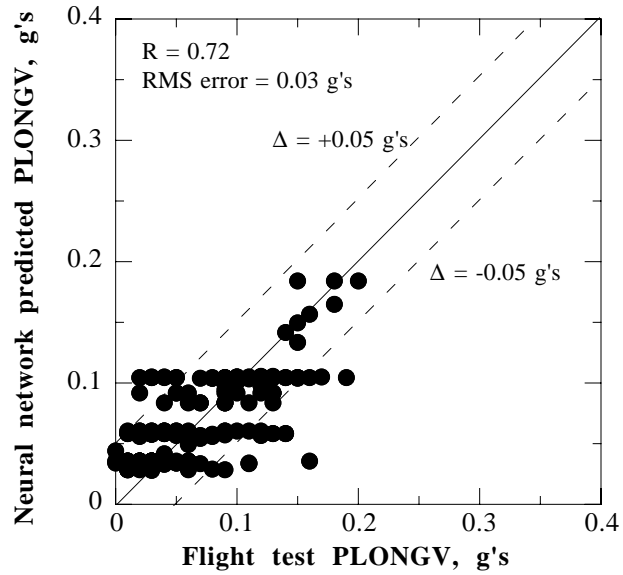
Fig. 28. PLONGV correlation using hub accelerations.

23
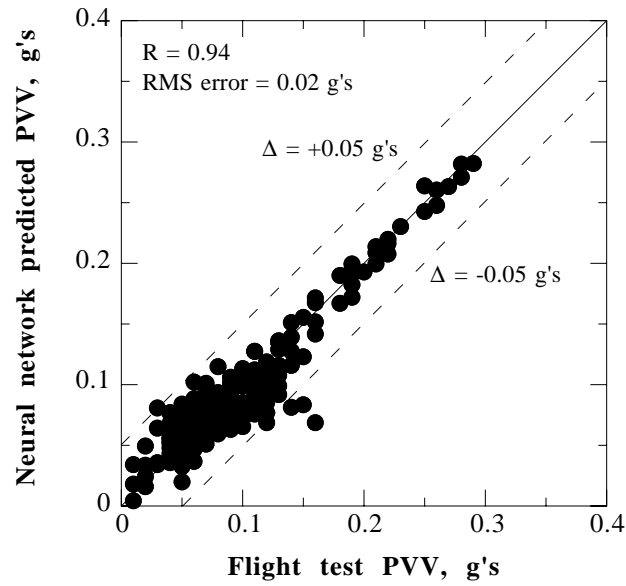
Fig. 29. PVV correlation using hub accelerations and advance ratio.
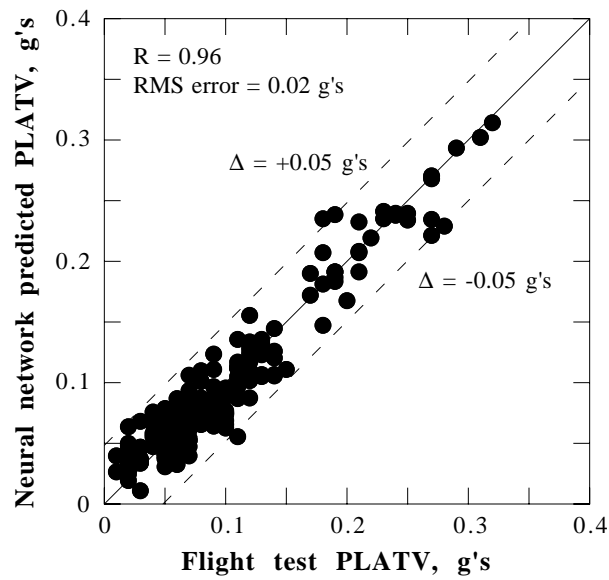
**Fig. 30. PLATV correlation using hub accelerations and advance ratio.**
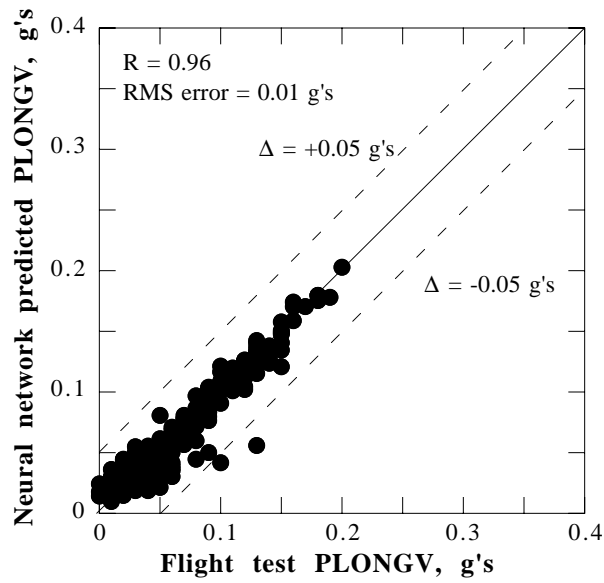
Fig. 31. PLONGV correlation using hub accelerations and advance ratio.
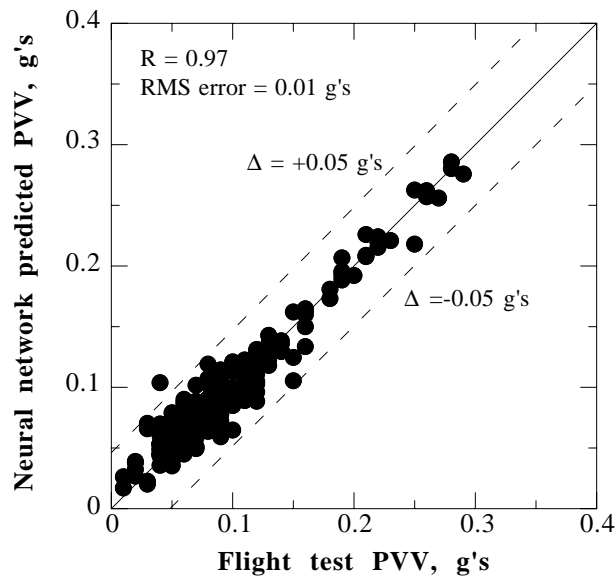
**Fig. 32. PVV correlation using hub accelerations along with advance ratio and gross weight.**
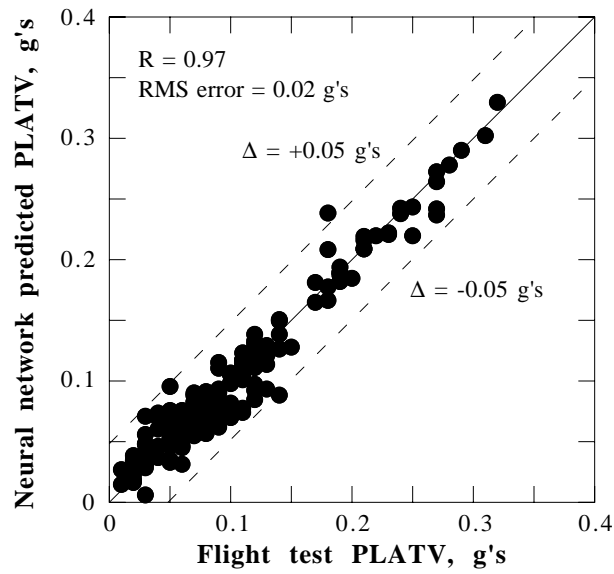
Fig. 33. PLATV correlation using hub accelerations along with advance ratio and gross weight.
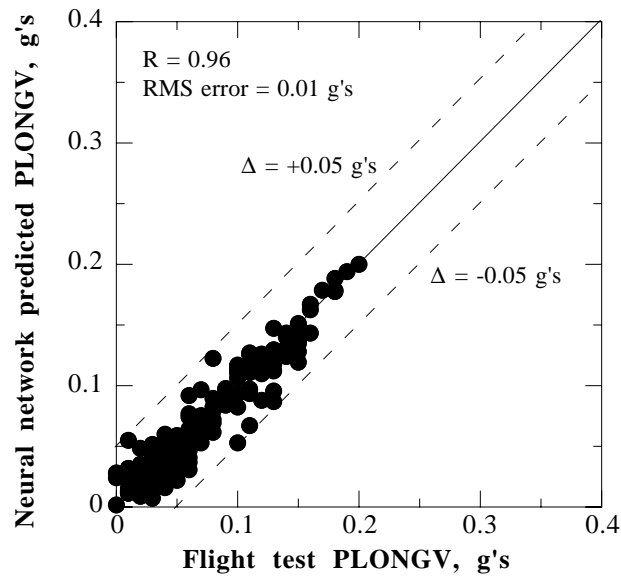
**Fig. 34. PLONGV correlation using hub accelerations along with advance ratio and gross weight.**
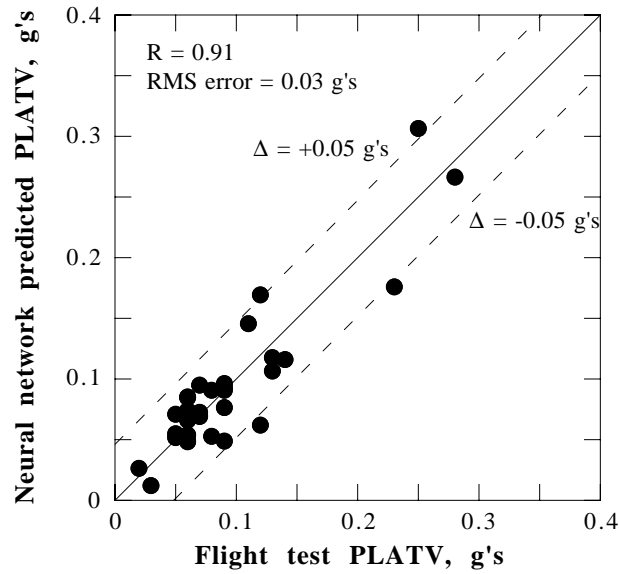
**Fig. 35a. Validation plot, six inputs including MEF, associated with Fig. 14.**
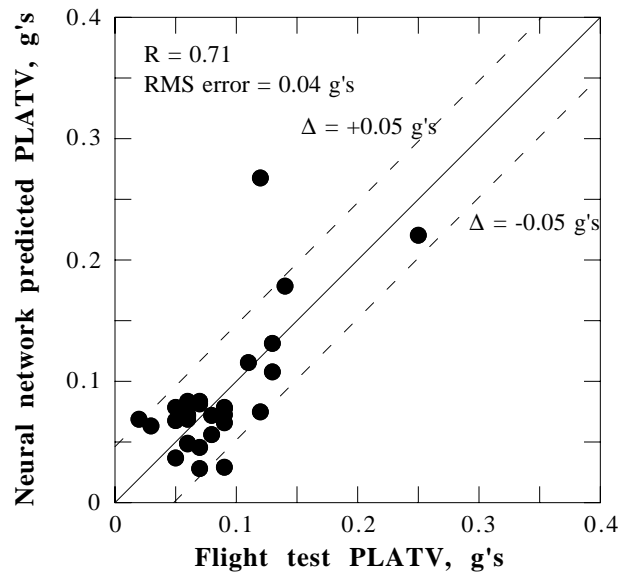
Fig. 35b. Validation plot, five inputs including hub accelerations, advance ratio and gross weight, associated with Fig. 33.
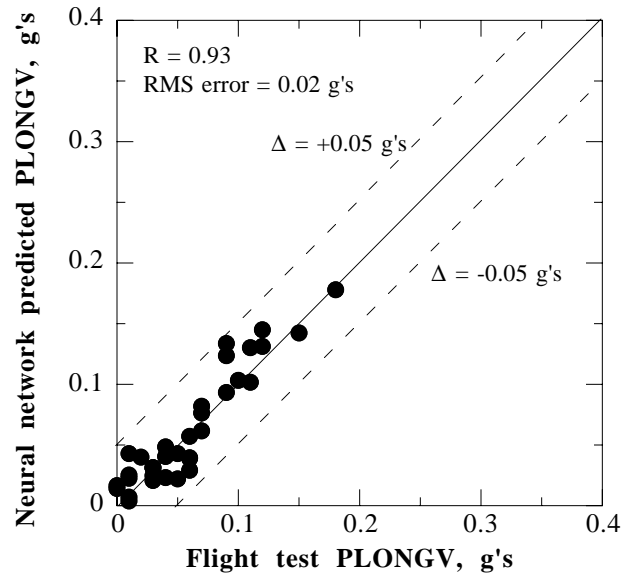
Fig. 36a. Validation plot, six inputs including MEF, associated with Fig. 15.
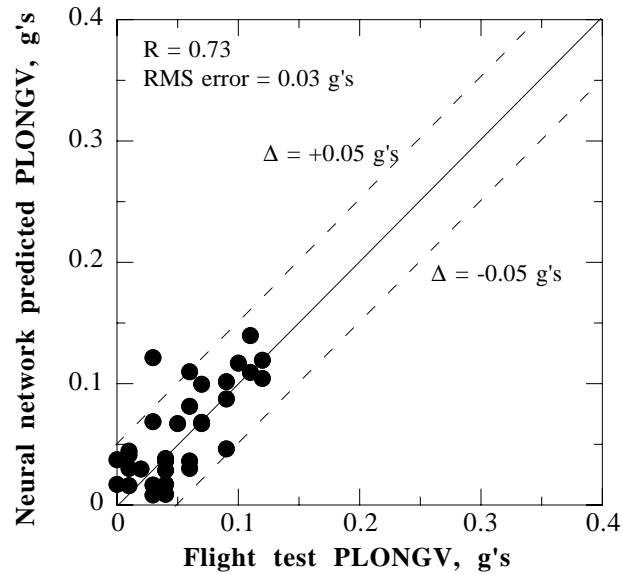

Fig. 36b. Validation plot, five inputs including hub accelerations, advance ratio and gross weight, associated with Fig. 34.